arXiv:1403.4163v1 [cond-mat.mes-hall] 17 Mar 2014

Inducing Lifshitz transition by extrinsic doping of surface bands in topological crystalline insulator $Pb_{1-x}Sn_xSe$

I. Pletikosić,[1,2,*] G. D. Gu,[2] and T. Valla[2]

[1] *Department of Physics, Princeton University, Princeton, NJ 08544, USA*
[2] *Condensed Matter Physics and Materials Science Department, Brookhaven National Laboratory, Upton, NY 11973, USA*

Narrow gap semiconductor $Pb_{1-x}Sn_xSe$ was investigated for topologically protected surface states in its rock-salt structural phase for x=0.45, 0.23, 0.15, and 0. Angle-resolved photoelectron spectroscopy of intrinsically *p*-doped samples showed clear indication of two Dirac cones, eccentric about the time-reversal invariant point $\bar{X}$ of the surface Brillouin zone for all but the x=0 sample. Adsorption of alkalies gradually filled the surface bands with electrons, driving the x>0 topological crystalline insulator systems through Lifshitz transitions, and from a hole- to electron-like Fermi surface. The electron-doped bands in x>0 samples exhibited the full configuration of the Dirac cones, also confirming electron-hole symmetry of the surface bands.

PACS numbers: 71.20.-b, 73.20.-r, 75.70.Tj, 79.60-i

Symmetries of physical systems govern many of their fundamental properties. In the case of topological insulators (TI), time-reversal symmetry provides protection of gapless surface states accommodated in the bulk band gap [1, 2]. These states appear as an odd number of Dirac cones crossing the Fermi level, and are known for their momentum-locked spin configuration, robustness against weak disorder, absence of elastic backscattering, and a myriad of exotic phenomena when interfaced with magnetism or superconductivity [3, 4].

A related class of materials, topological crystalline insulators (TCI), owe the protection of their gapless surface bands to crystal inversion symmetries [5]. The prediction of such states came from symmetry considerations on a family of IV-VI semiconductors with strong spin-orbit coupling, $Pb_{1-x}Sn_x$(Te,Se) [6, 7], long known for the inversion of the bulk band structure at two extremal compositions x [8–10]. Even though the surface states of these semiconductors become topologically nontrivial only when uniaxial deformation is introduced [11], it was found that the mirror symmetry with respect to the [110] plane gives necessary protection to spin-momentum locked states localized at their (001), (111) or (110) surfaces. Surface states at (001), in which the rock-salt crystals naturally cleave, comprise of four Dirac cones centered slightly off the surface Brillouin zone boundary, near the $\bar{X}$ point ($k_{x|y} = 0.73\,\text{Å}^{-1}$, $k_{y|x} = 0$) on the mirror-symmetric line $\bar{\Gamma}$–$\bar{X}$–$\bar{\Gamma}$. These states have been observed in a recent series of angle-resolved photoemission (ARPES) studies [12–16]. It was found that (001) surface states of $Pb_{1-x}Sn_xTe$ are topologically trivial [15] and gapped [12] for $x < 0.3$, but develop to two Dirac cones moving away from $\bar{X}$ for $x > 0.3$, all up to $x = 1$ [15]. Also, clear manifestations of TCI spin-locked states have been found for the (001) surface of $Pb_{0.73}Sn_{0.27}Se$, as well as their temperature dependent transition from topological to trivial [14, 16]. All these lack a precise mapping of the low-energy configuration of the surface bands, which is a crucial element in determining quasiparticle scattering patterns and possible scattering protections [17, 18].

A peculiar feature in the electronic structure of these states is the existence of so called Lifshitz points, where the change in topology of constant energy contours occurs. By varying the filling of the surface states, the Lifshitz transitions could, in principle, be induced, with interesting consequences on surface transport. This, and a wealth of exotic features, from extremely high surface mobilities to ferroelectricity and superconductivity, but also the possibility of their tuning by strain, doping or alloying, make these materials worth exploring both from the fundamental perspective and for various applications.

Here we investigate (001) surface states of $Pb_{1-x}Sn_xSe$ over a range of compositions for which the crystals grow in rock-salt structure. We set the lower limit on x at which the transition from TCI to trivial surface states occurs, and give a precise experimental characterization of the two interlocking Dirac cones. We also show that initially *p*-type surfaces can be gradually turned into *n*-type by adsorbing electron donors, demonstrating the possibility of a transformation of the Fermi surface topology through the Lifshitz transition.

Single crystal ingots of $Pb_{1-x}Sn_xSe$ were grown in a custom built floating zone apparatus from the stoichiometric melt of high purity (5N) constituent elements. Samples of a few cubic millimeters were cut from the ingots and cleaved *in situ* for the experiments.

ARPES measurements have been conducted at the U13 beamline ($h\nu$ from 17 to 22 eV) of the National Synchrotron Light Source at Brookhaven National Laboratory using a Scienta 2002 analyzer with an overall energy resolution of 15 meV and angular resolution <0.2° . Brillouin zone mapping was accomplished by polar angle rotation, perpendicularly to the analyzer slit, in steps of 0.5°. Liquid helium was used to cool the samples down to 10 K.

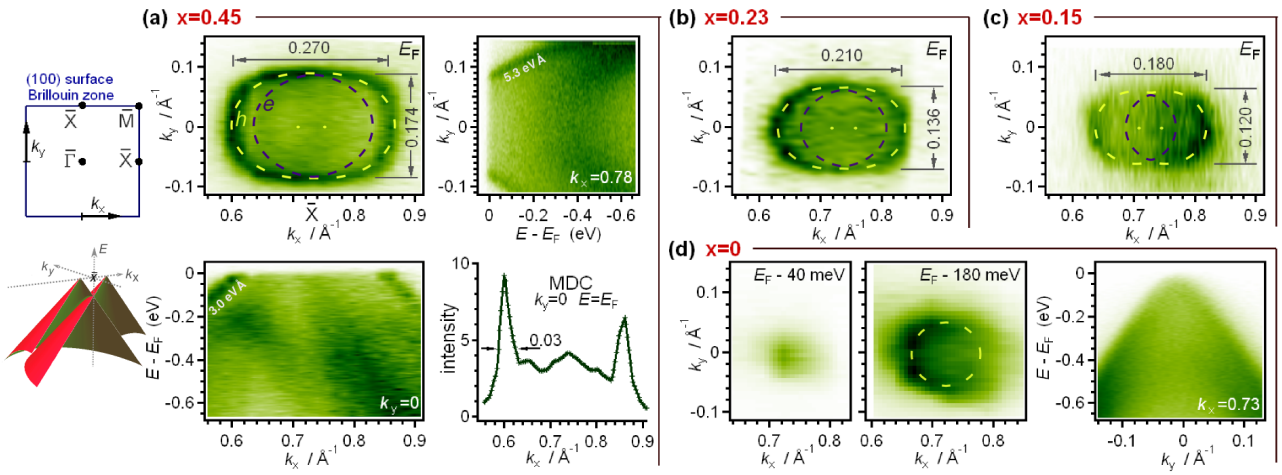

Figure 1: (color online) ARPES intensity maps taken at 18 K from the (001) surface of intrinsically p-doped $Pb_{1-x}Sn_xSe$ samples in the vicinity of the $\bar{X}$ point of the surface Brillouin zone ($k = 0.73\,\text{Å}^{-1}$) for four different compositions x. (a) Fermi surface, band dispersions along k_y (at $k_x = 0.78\,\text{Å}^{-1}$) and k_x(at $k_y = 0$), and momentum distribution curve (MDC) of the bands close to the Fermi level (E_F) along the $\bar{\Gamma}$–$\bar{X}$–$\bar{\Gamma}$ direction for $x = 0.45$; (b) and (c) constant energy maps for $x = 0.23$ and $x = 0.15$ samples at the Fermi energy; (d) constant energy maps for the $x = 0$ sample 40 and 180 meV below the Fermi level, and the band dispersion map along k_y at $\bar{X}$. Dashed lines added to the constant energy maps represent assumed band configuration of two Dirac cones slightly eccentric about $\bar{X}$ (calculated by a formula from Ref. 19). Electron/e and hole/h pockets are separately marked.

ARPES intensity maps for $x > 0$, Figs. 1(a)–(c), show a region of higher intensity centered at $\bar{X}$, encircled by hole-like bands, and low background intensity beyond. Unlike the inner, broad and mostly featureless bands, the outer bands are sharp, having the Fermi level momentum distribution curve (MDC) width at half maximum of $0.03\,\text{Å}^{-1}$. These bands show no dependence on the excitation energy, which by not having out-of-surface momentum k_z as a quantum number, signifies their surface localization (cf. Fig. S1 in Supplemental Material [20]). Band dispersion spectra, like the two shown in Fig. 1(a) taken along and perpendicular to the $\bar{\Gamma}$–$\bar{X}$–$\bar{\Gamma}$ direction, exhibit linear bands in all directions over the energy region probed.

The elongated shape of the constant energy cuts of the outer (surface) states points to their origin in two interlocking Dirac cones slightly displaced from $\bar{X}$ along the $\bar{\Gamma}$–$\bar{X}$–$\bar{\Gamma}$ direction, as already found for $Pb_{0.77}Sn_{0.23}Se$ [14] or $Pb_{1-x}Sn_xTe$ [12, 13, 15]. And indeed, the $k_x - k_y$ constant energy maps, as those shown in Fig. 1 for the Fermi energy, are easily fitted by the contours of a model band dispersion given by Liu *et al.* [19], with the parameters adjusted in order to reproduce the observed band velocities (v_x, v_y) and the overall shape governed by (m, δ) which parametrize intervalley scattering at the lattice scale. Both sets of parameters greatly differ from those that Liu *et al.* obtained by fitting to density-functional *ab initio* bands (Figure 3 in Liu et al. [19], $m = 70$, $\delta = 26$, $v_x = 2.4$, $v_y = 1.3$). While our values of $m = 6 \pm 3\,\text{meV}$, $\delta = 68 \pm 3\,\text{meV}$ and $v_y = 2.8 \pm 0.3\,\text{eVÅ}$ (in the geometry used by Liu *et al.*) appear to be universal for all the fitted bands, velocity v_x in the direction perpendicular to $\bar{\Gamma}$–$\bar{X}$–$\bar{\Gamma}$ had to be tuned from 5.3 eVÅ for the $x = 0.45$ sample, to 4.4 eVÅ for $x = 0.23$, and to 3.5 eVÅ for the $x = 0.15$ sample. This variation probably indicates that the model is only applicable to the parts of the bands close to the Dirac points, and that considerable warping takes place at energies farther away. As we will see below, our values for m and δ result in highly circular constant energy contours, in contrast to distorted contours obtained in most theoretical considerations [19, 21, 22].

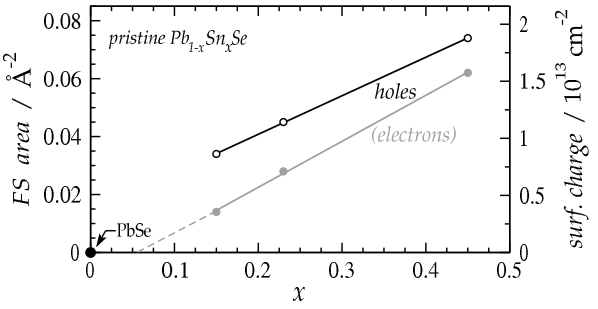

Figure 2: Tin content x dependence of hole and electron pocket Fermi surface areas for surface states in intrinsic p type $Pb_{1-x}Sn_xSe$.

From Figs. 1(a)–(c) it is obvious that the Fermi surfaces (FS) of the $x > 0$ samples shrink in size with decreasing Sn content x. Taking the measures of the contours, we calculated the FS areas for the hole and electron pockets in the first surface Brillouin zone and plotted them in Fig. 2. The dependence on x is manifestly linear.

A small variation among the samples cut from the same ingot was found, as the intrinsic doping (thus the Fermi surface size) is known to be dependent on the growth conditions, defects present, etc. [9, 14, 23, 24] As we will explain below, only the hole charge contained in surface bands(right axis in Fig. 2), has physical relevance in our samples, the charge from the electron pockets being delocalized in the bulk. Extrapolating the derived electron pocket FS size to zero, the composition of $x \approx 0.05$ would correspond to a point of Lifshitz transition in the pristine sample. Before reaching that point, however, a subtle quantum phase transition might occur that would make the bands topologically trivial.

Comparison of the spectra for $x > 0$ in Figs. 1(a)–(c) with the spectra for PbSe ($x = 0$) in Fig. 1(d), where a single cone isotropic around X is found, leaves no doubt that all three $x > 0$ samples are topological crystalline insulators. This has been further elucidated by extrinsic doping of the bands, which unveiled the upper Dirac cones and also made all their branches visible.

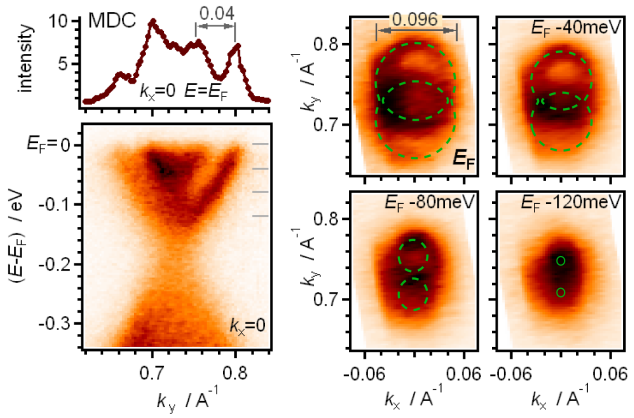

Figure 3: (color online) ARPES intensity maps from the electron doped (001) surface of $Pb_{0.85}Sn_{0.15}Se$ ($x = 0.15$). The doping was achieved by rubidium adsorption at 18 K. Momentum distribution curve (MDC) is from the band dispersion spectrum taken along the k_y direction in the vicinity of $\bar{X}$ ($k_x = 0$). Constant energy cuts of the two Dirac cones eccentric about $\bar{X}$, made at the Fermi level (E_F) and 40, 80, and 120 meV below are shown on the right.

It is well known that alkali atoms when adsorbed onto a surface give away their electrons, the charge transfer to the substrate being dependent on the coverage. This has been demonstrated as a very effective way of electron-doping of surfaces of TIs and tuning of the band filling, similar to the gate-doping in transport devices [25]. Here, upon a gradual lowering of the electronic bands, saturation appears and no further doping is possible. Given its low intrinsic p-doping, the $x = 0.15$ sample was easiest to dope with electrons, exposing most of the electronic structure above the Dirac point. A band dispersion ARPES spectrum on the left of Fig. 3 shows a cut through the electronic structure of a Rb covered $x = 0.15$ sample along the $\bar{\Gamma}$–$\bar{X}$–$\bar{\Gamma}$ high-symmetry line. For the sake of a precise momentum-space mapping, it was taken at an elevated tilt angle—along the k_y direction. The spectrum unambiguously presents a cross-section of two Dirac cones shifted by 0.04 Å^{-1} along the $\bar{\Gamma}$–$\bar{X}$ direction in momentum space, one cone showing brighter than the other. Their apex is found at 0.14 eV below the Fermi level. Compared to the 0.16–0.28 Å^{-1} cone separation in $Pb_{1-x}Sn_xTe$ [12, 15], the separation of 0.04 Å^{-1} in $Pb_{1-x}Sn_xSe$ makes the analysis of the tangled bands more difficult. Only due to relatively sharp surface bands, having the width at half maximum as low as 0.022Å^{-1}, we were able to determine the details of their configuration with sufficient precision. Constant energy maps of the region of momentum space around $\bar{X}$ show a pattern of two circles always centered about the same points. Slices of the cones at four different energies referenced to the Fermi level, displayed on the right side of Fig. 3, have been fitted by the contours of a theoretical model by Liu *et al.* [19] (using $m = 6$ meV, $\delta = 67$ meV, and $v_x = 2.9$ eVÅ, $v_y = 3.1$ eVÅ). Note that these parameters are very similar to those needed to fit the pristine bands, suggesting that the surface state is particle-hole symmetric. The contours start at the Dirac point, roughly 140 meV below the Fermi level, like two separate circular electron pockets, but then go to a topologically distinct configuration around -80 meV, in which the outer contour forms an electron pocket while the inner, interlocked part, forms a hole pocket. The transition between the two configurations is easy to induce, as the electron doping by alkali deposition can continuously sweep the chemical potential through the portions of the lower and upper Dirac cones.

To establish the relation between the upper and lower bands, we superimpose in Fig. 4(a) the band dispersion images taken from the intrinsically p-doped $x = 0.15$ sample along the $\bar{\Gamma}$–$\bar{X}$–$\bar{\Gamma}$ direction, and the same sample in the highest n-doping achieved by rubidium adsorption at 10 K. Having the two lower bands extended by dashed lines, a position can be found where they agree with two bands of the upper cones. An extension of the remaining two upper bands to lower energies shows their coincidence with the area of increased intensity that has been ascribed to photoemission from the bulk. By having a possibility of bulk propagation, these states do not show up as distinct surface bands. This is why the inner, interlocked bands traced by the theoretical contours in Fig. 1 were not resolved on the Fermi surface maps of any of the $x > 0$ samples. The same applies to the lower bands in doped samples: as the energy shift by doping of the surface and bulk bands is not the same, these states probably overlap with the bulk states, therefore losing their surface localization. The upper Dirac cones of the doped samples are outside of the region of the bulk bands, and are all clearly resolved.

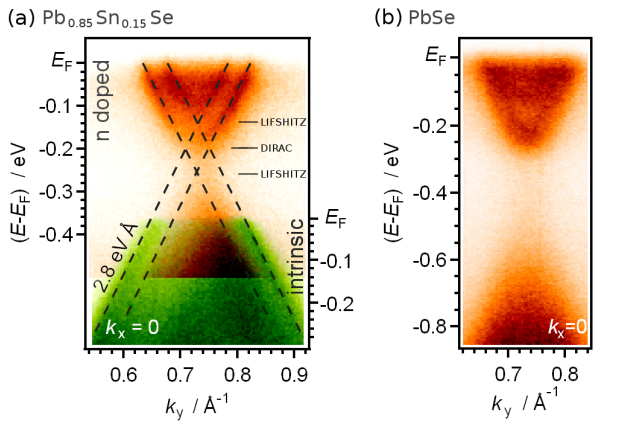

Figure 4: (color online) (a) ARPES spectrum showing highly n-doped surface bands in $Pb_{0.85}Sn_{0.15}Se$ ($x = 0.15$) realized by rubidium adsorption at 10 K (orange) is superimposed onto the spectrum of the pristine, intrinsically p-doped sample (green). Dashed lines match the four bands of the upper Dirac cones and two bands of the lower cones. (b) ARPES spectrum of highly doped bands of PbSe. All spectra were taken along the $\bar{\Gamma}$–$\bar{X}$–$\bar{\Gamma}$ direction. Note different energy scales in (a) and (b).

The overlay of the two spectra makes possible assessing their doping levels with respect to the Dirac point: the pristine sample exhibits a 170 meV p-doping, while the sample of the highest extrinsic doping shows surface bands lowered by 190 meV. We have thus made a transition from a hole-like Fermi surface of the pristine $x = 0.15$ sample, to a similar size electron-like Fermi surface by *in-situ* doping. On the way, surface bands went through two Lifshitz transitions, 67 meV on either side of the Dirac crossing. Similar position of the Lifshitz transition can be inferred from a tunneling study by Okada *et al.* [26] They interpret the maximum in dI/dV curves ± 40 meV from the Dirac point as the position of a van Hove singularity in the density of states. This places the Lifshitz points at ± 70 meV ($E_{DP2\pm}$ in Fig. 1D, Ref. 26).

We note that the two outer bands of highly doped $Pb_{0.85}Sn_{0.15}Se$ samples (Figs. 3 and 4; also raw spectra in Supplemental Material [20], Fig. S2) show an abrupt change of velocity, approximately at the level of the Lifshitz crossing. This has not been captured by the $k \cdot p$ formula by Liu *et al.* [19] which gives strikingly linear bands, nor a more elaborate Hamiltonian by Fang *et al.* [22] was able to reproduce the kink in our previous work, Ref. 18, tending to bend the bands in the direction opposite of the observed. One should therefore consider if the change in the band topology at the Lifshitz transition or the nearby van Hove singularity in the density of states coming from the band minimum along $\bar{X}$–$\bar{M}$ marks an onset of an interaction that would renormalize the bands. This, as well as structural mirror-symmetry breaking proposed by Okada *et al.* [26], could lead to mass acquisition in the Dirac bands.

In a final test, the $x = 0$ sample was electron doped by rubidium adsorption. As Fig. 4(b) shows, no double-cone structure was found, but a single upper surface state with a curved apex, separated from the lower states by a gap of at least 200 meV. Similar gapped states were found in topologically trivial $Pb_{0.8}Sn_{0.2}Te$ [12]. Interestingly enough, the $x = 0$ case appears to be a limiting case of the two spin-locked Dirac cones coalescing into one as the Sn content is being reduced. Trends are clear: the cones in $Pb_{1-x}Sn_xTe$ were found approaching each other from 0.26 Å^{-1} at x=0.5 to 0.16 Å^{-1} at x=0.3 [15]; in $Pb_{1-x}Sn_xSe$, a separation of 0.054 Å^{-1} found for x=0.23 [14] reduces to 0.04 Å^{-1} for x=0.15. It is interesting to note that the surface doping does not affect the eccentricities or any other aspect of the surface electronic structure, implying that these properties are determined by the bulk and that the extrinsic doping does not break any relevant crystal symmetries.

To summarize, (001) surface states of $Pb_{1-x}Sn_xSe$ appeared as two Dirac cones eccentric about the $\bar{X}$ point of the surface Brillouin zone for x=0.45, 0.23, and 0.15, but a single cone for x=0, indicating a transition from topologically protected to trivial states at Sn content lower than 0.15, in contrast to $Pb_{1-x}Sn_xTe$ system which ceases to be a TCI already at x=0.3 [15]. Electron doping by rubidium adsorption drove the system through Lifshitz transitions and showed that, aside from the differences in the overlap with the bulk bands, the surface states are particle-hole symmetric.

This work was supported by ARO MURI program, grant W911NF-12-1-0461, and US Department of Energy, Office of Basic Energy Sciences, contract no. DE-AC02-98CH10886.

* Electronic address: ivop@princeton.edu

[1] S. Murakami, N. Nagaosa, and S.-C. Zhang, Physical Review Letters **93**, 156804 (2004), ISSN 0031-9007, URL http://link.aps.org/doi/10.1103/PhysRevLett.93.156804.

[2] C. L. Kane and E. J. Mele, Physical Review Letters **95**, 146802 (2005), ISSN 0031-9007, URL http://link.aps.org/doi/10.1103/PhysRevLett.95.146802.

[3] M. Z. Hasan and C. L. Kane, Reviews of Modern Physics **82**, 3045 (2010), 1002.3895, URL http://link.aps.org/doi/10.1103/RevModPhys.82.3045.

[4] X.-L. Qi and S.-C. Zhang, Reviews of Modern Physics **83**, 1057 (2011), ISSN 0034-6861, URL http://link.aps.org/doi/10.1103/RevModPhys.83.1057.

[5] L. Fu, Physical Review Letters **106**, 106802 (2011), URL http://link.aps.org/doi/10.1103/PhysRevLett.106.106802.

[6] T. H. Hsieh, H. Lin, J. Liu, W. Duan, A. Bansil, and L. Fu, Nature communications **3**, 982 (2012), URL http://dx.doi.org/10.1038/ncomms1969.

[7] B. Volkov and O. Pankratov, JETP Lett **42**, 145

(1985), URL http://www.jetpletters.ac.ru/ps/1420/article_21570.pdf?ref=Guzels.TV.

[8] A. Strauss, Physical Review **157**, 608 (1967), URL http://prola.aps.org/abstract/PR/v157/i3/p608_1.

[9] R. Dalven, Infrared physics **9**, 141 (1969), URL http://adsabs.harvard.edu/abs/1969InfPh...9..141D.

[10] A. Calawa, J. Dimmock, T. Harman, and I. Melngailis, Physical Review Letters **172**, 242 (1969), URL http://www.ncbi.nlm.nih.gov/pubmed/23476080http://link.aps.org/doi/10.1103/PhysRevLett.23.7.

[11] L. Fu and C. Kane, Physical Review B **76**, 045302 (2007), URL http://link.aps.org/doi/10.1103/PhysRevB.76.045302.

[12] S.-Y. Xu, C. Liu, N. Alidoust, M. Neupane, D. Qian, I. Belopolski, J. D. Denlinger, Y. J. Wang, H. Lin, L. A. Wray, et al., Nature communications **3**, 1192 (2012), URL http://www.ncbi.nlm.nih.gov/pubmed/23149737.

[13] Y. Tanaka, Z. Ren, T. Sato, K. Nakayama, S. Souma, T. Takahashi, K. Segawa, and Y. Ando, Nature Physics **8**, 800 (2012), URL http://www.nature.com/doifinder/10.1038/nphys2442.

[14] P. Dziawa, B. J. Kowalski, K. Dybko, R. Buczko, A. Szczerbakow, M. Szot, E. Lusakowska, T. Balasubramanian, B. M. Wojek, M. H. Berntsen, et al., Nature materials **11**, 1023 (2012), URL http://www.ncbi.nlm.nih.gov/pubmed/23023551.

[15] Y. Tanaka, T. Sato, K. Nakayama, S. Souma, T. Takahashi, Z. Ren, M. Novak, K. Segawa, and Y. Ando, Physical Review B **87**, 155105 (2013), URL http://link.aps.org/doi/10.1103/PhysRevB.87.155105.

[16] B. M. Wojek, R. Buczko, S. Safaei, P. Dziawa, B. J. Kowalski, M. H. Berntsen, T. Balasubramanian, M. Leandersson, A. Szczerbakow, P. Kacman, et al., Physical Review B **87**, 115106 (2013), URL http://link.aps.org/doi/10.1103/PhysRevB.87.115106.

[17] I. Zeljkovic, Y. Okada, C.-Y. Huang, R. Sankar, D. Walkup, W. Zhou, M. Serbyn, F. Chou, W.-F. Tsai, H. Lin, et al., arXiv preprint arXiv:1312.0164 (2013), 1312.0164, URL http://arxiv.org/abs/1312.0164.

[18] A. Gyenis, I. K. Drozdov, S. Nadj-Perge, O. B. Jeong, J. Seo, I. Pletikosić, T. Valla, G. D. Gu, and A. Yazdani, Physical Review B **88**, 125414 (2013), ISSN 1098-0121, URL http://link.aps.org/doi/10.1103/PhysRevB.88.125414.

[19] J. Liu, W. Duan, and L. Fu, Physical Review B **88**, 241303 (2013), ISSN 1098-0121, URL http://link.aps.org/doi/10.1103/PhysRevB.88.241303.

[20] See Supplemental Material at [URL will be inserted by publisher] for excitation energy dependence and raw spectra of electron doped samples.

[21] S. Safaei, P. Kacman, and R. Buczko, arXiv preprint arXiv:1303.7119 pp. 1–8 (2013), URL http://arxiv.org/abs/1303.7119.

[22] C. Fang, M. J. Gilbert, S.-Y. Xu, B. A. Bernevig, and M. Z. Hasan, Physical Review B **88**, 125141 (2013), ISSN 1098-0121, URL http://link.aps.org/doi/10.1103/PhysRevB.88.125141.

[23] J. Melngailis, T. Harman, and W. Kernan, Physical Review B **5**, 2250 (1972), URL http://prb.aps.org/abstract/PRB/v5/i6/p2250_1.

[24] J. Dixon and G. Hoff, Physical Review B **3** (1971), URL http://prb.aps.org/abstract/PRB/v3/i12/p4299_1.

[25] T. Valla, Z.-H. Pan, D. Gardner, Y. S. Lee, and S. Chu, Physical Review Letters **108**, 117601 (2012), ISSN 0031-9007, URL http://link.aps.org/doi/10.1103/PhysRevLett.108.117601.

[26] Y. Okada, M. Serbyn, H. Lin, D. Walkup, W. Zhou, C. Dhital, M. Neupane, S. Xu, Y. J. Wang, R. Sankar, et al., Science (New York, N.Y.) **341**, 1496 (2013), ISSN 1095-9203, URL http://www.ncbi.nlm.nih.gov/pubmed/23989954.